

Morphology and rheology of compatibilized polymer blends: Diblock compatibilizers vs crosslinked reactive compatibilizers

Candice L. DeLeo and Sachin S. Velankar^{a)}

*Department of Chemical Engineering, University of Pittsburgh,
Pittsburgh, Pennsylvania 15261*

(Received 20 February 2008; final revision received 4 September 2008)

Synopsis

Reactive compatibilization is commonly used when blending immiscible homopolymers. The compatibilizers formed from the interfacial coupling of two types of reactive chains often have a graft copolymer architecture. Here we consider the case where both reactive chains are multifunctional, leading to a crosslinked copolymer at the interface. Experiments were conducted on a model blend of ~30% polydimethylsiloxane drops in a polyisoprene matrix. Compatibilizer was formed by an interfacial reaction between amine-functional polydimethylsiloxane and maleic anhydride-functional polyisoprene. Both species were multifunctional, and therefore capable of interfacial crosslinking. Optical microscopy showed some unusual features including drop clusters, nonspherical drops, and some drops with apparently nonsmooth surfaces. All these features suggest that a crosslinked “skin” covers the interface of the drops. Rheologically, the reactively compatibilized blend showed gel-like behavior in oscillatory experiments, enhanced viscosity and elastic recovery at low stresses, and strong viscosity overshoots in creep experiments, all of which are likely attributable to drop clustering. At the highest stress studied (400 Pa), the viscosity of the reactively compatibilized blend is comparable to that of a similar blend compatibilized by diblock copolymer. This suggests that, in practical processing operations that occur at even higher stresses, interfacial crosslinking by multifunctional chains will not adversely affect processability. © 2008 The Society of Rheology. [DOI: 10.1122/1.2995857]

I. INTRODUCTION

Compatibilizers are commonly used to promote blending of immiscible homopolymers. Numerous researchers have used premade diblock copolymers in studies of immiscible blends principally because the structure of the compatibilizer is known precisely, and the amount of compatibilizer present in the blend can be controlled exactly. However, industrially it is much more common to generate a compatibilizer by an interfacial chemical reaction between reactive polymers. Some homopolymers are inherently reactive, e.g., polyamides have primary amine end groups and polyesters have carboxylic acid or alcohol end groups. In other cases, reactive polymers may be added to otherwise inert phases specifically to promote reactive compatibilization. The reactive groups then arrive at the interface by diffusion, usually aided by the flow applied by the blending operation, resulting in compatibilizer formation at the interface.

^{a)}Author to whom correspondence should be addressed; electronic mail: velankar@pitt.edu

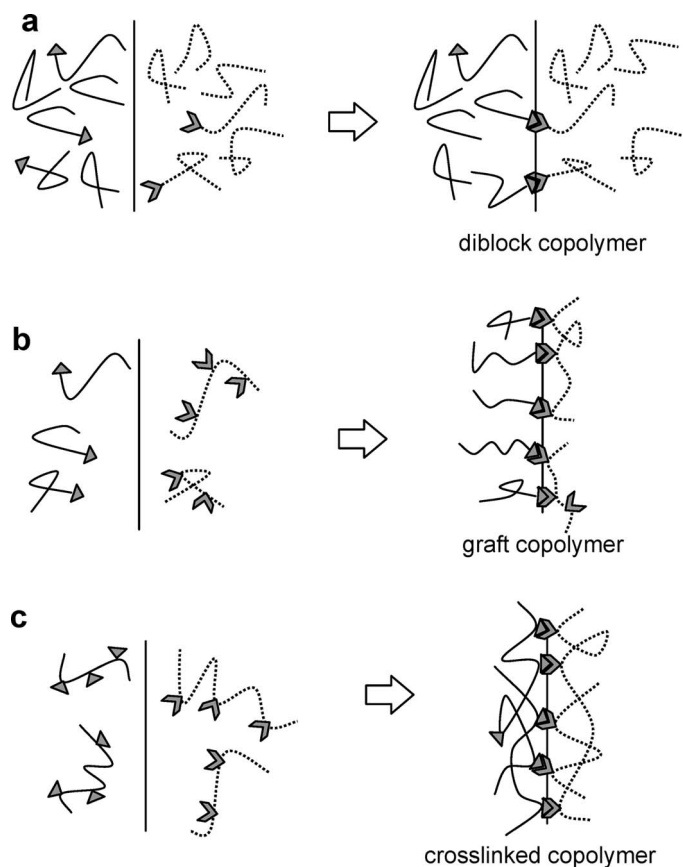


FIG. 1. Reactive compatibilization leading to various compatibilizer architectures at the interface. (a) Both reactive species are linear, mono-end-functional, resulting in diblock compatibilizers, (b) one reactive species is linear mono-end-functional, whereas the other is a linear multifunctional polymer giving graft architecture, (c) both reactive species are multifunctional, resulting in a crosslinked interface. Note that in addition to the reactive species, unreactive chains may be present in both phases. These are shown explicitly only in (a).

The architecture of the compatibilizer formed at the interface is determined mainly by the structure of the reactive chains. Figure 1 illustrates some possible architectures; this list is not comprehensive, and other possible architectures are mentioned below.

The simplest possibility is of linear mono-end-functional chains reacting to form a diblock copolymer [Fig. 1(a)]. Due to the conceptual simplicity of diblock formation, reactively generated diblocks are popular in laboratory studies of the kinetics and mechanisms of reactive compatibilization [Cernohous *et al.* (1997); Schulze *et al.* (2000); Yin *et al.* (2003); Jeon *et al.* (2004); Kim *et al.* (2005)]. However, reactive generation of diblocks is not a common industrial occurrence, although the review by Koning *et al.* (1998) has cited some examples from the patent literature [Aycock and Ting (1986, 1987); Brown *et al.* (1992)]. Variations of diblock formation, e.g., three or four arm stars formed from mono-mid-functional chains, are also possible, but not illustrated in Fig. 1.

The second possibility of reactive compatibilization is that illustrated in Fig. 1(b), where an end-functional chain in one phase reacts with a multifunctional chain in the other to form a graft copolymer at the interface. Numerous reactively generated compatibilizers are graft copolymers, and for this reason, in some of the literature, “grafting” is

virtually synonymous with reactive compatibilization. One heavily studied example is of polyamides, which have primary amine end groups, reacting with maleated polyolefins [see Sec. B 5 of [Datta and Lohse \(1996\)](#) for numerous citations]. This reaction led to the commercialization of supertough nylon. Another commonly studied example is of polyesters, which have acid or hydroxy end groups, reacting with epoxy-functional polyolefins [[Lee et al. \(1994\)](#); [Hale et al. \(1999\)](#); [Martin et al. \(2001\)](#)]. Graft copolymers can also be formed from reactions such as transesterification [[Wildes et al. \(1999\)](#)] or acidolysis [[Zhang et al. \(2000\)](#)] that involve pendant groups.

The above two cases of Figs. 1(a) and 1(b) have the notable feature that at least one of the reactive species was monofunctional. There are, however, numerous cases in which both reactive species are multifunctional. In such cases, the compatibilizer is not expected to be a graft copolymer, but instead a crosslinked network as illustrated in Fig. 1(c). The distinction between a graft architecture and a crosslinked one is not a sharp one. When the functionality of the reactive species only slightly exceeds one reactive group per chain, a highly branched copolymer architecture is expected. With increasing functionality, a true network structure is expected. Some examples of such reactive compatibilization with two multifunctional species include blends of oxazoline-functional polystyrene and maleated ethylene-propylene [[Sundararaj and Macosko \(1995\)](#); [Lin et al. \(2005\)](#)], blends of acid-functional polymer and polyvinylpyridine (in which the species react by acid-base interactions) [[Beretta and Weiss \(1987\)](#); [Beck Tan et al. \(1996\)](#)], polyethylene/polystyrene blends with a Friedel Crafts reaction between the two species [[Sun et al. \(1998\)](#)], and several studies of blends of glycidylmethacrylate-functional polymers with acid-functional polymers [[Liu et al. \(1993\)](#); [Chen et al. \(1996\)](#); [Kim et al. \(1997\)](#); [Tselios et al. \(1998\)](#)]. Other similar examples can be found in the literature and in the citations of reviews [[Datta and Lohse \(1996\)](#); [Koning et al. \(1998\)](#); [Baker et al. \(2001a\)](#)].

In summary, compatibilization by the interfacial reaction of two multifunctional species is not uncommon in the literature. Remarkably, however, none of the above publications explicitly comment on the possibility that the two multifunctional reactive species can lead to a crosslinked interface. Indeed, in occasional such papers, the compatibilizer is even referred to as a “graft copolymer” when in fact the multifunctional nature of the reacting species makes a graft copolymer architecture unlikely. Interestingly, even some cases that are generally regarded as graft copolymer compatibilizers do not have a strictly graft architecture. For example, with polyamides, some fraction of the chains must have two amine groups, and hence, even the commonly studied polyamide/maleated polyolefin case may allow some degree of interfacial crosslinking. This was recognized in studies by [Paul et al.](#) on blends of maleated rubbers and polyamides [[Oshinski et al. \(1992\)](#); [Takeda et al. \(1992\)](#); [Majumdar et al. \(1994\)](#); [Oshinski et al. \(1996\)](#)]. They noted that blends based on nylon-6,6 sometimes gave large and complex rubber particles, whereas those based on nylon-6 or nylon-12 generally resulted in small and spherical particles. This was attributed to the fact that while materials such as nylon-6 are strictly monofunctional, some chains of nylon-6,6 are difunctional, and hence, capable of crosslinking.

The goal of this paper is to specifically focus on blends with multifunctional reactive compatibilization that leads to interfacial crosslinking. Our experimental approach uses “model” blends: blends of polymers chosen for their experimentally convenient attributes such as being liquid at room-temperature, transparent, inexpensive, and readily available. Since the bulk phases of the blends had simple rheological properties, all non-Newtonian behavior can be unambiguously attributed to interfacial phenomena. Model blends compatibilized with diblock copolymers have yielded many insights into the role of the diblock in affecting breakup and coalescence, immobilizing the interface, and causing interfacial viscoelasticity [[Hu et al. \(2000\)](#); [Hu and Lips \(2003\)](#); [Van Hemelrijck et al.](#)

TABLE I. Materials used.

Material	MW (g/mol)	$\eta_{25\text{ }^\circ\text{C}}$ (Pa s)	Composition	Supplier
PI LIR30	29 000 ^b	131	100% PI	Kuraray
PIMA	25 000 ^b	1700	1.5% MA ^b	Aldrich
PDMS	135 600 ^a	96	100% PDMS	Rhodia
PDMS*	5000 ^b	0.1	2–3% NH ₂ ^b	Gelest
PI- <i>b</i> -PDMS	PI: 26 000; PDMS: 27 000		48% PI	KUL ^c

^aWeight-average molecular weight estimated from known viscosity-MW relationship.

^bValue quoted by supplier.

^cSupplied by the Laboratory of Applied Rheology, K.U. Leuven.

(2004); Velankar *et al.* (2004); Van Hemelrijck *et al.* (2005); Wang and Velankar (2006); Yoon *et al.* (2007); Martin and Velankar (2008)]. In this paper, we employ model compatibilized blends to examine the effect of multifunctional reactive compatibilizers that crosslink the interface.

II. MATERIALS AND METHODS

Various properties of all materials used are listed in Table I.

The principal components of the blends are polyisoprene (PI, Kuraray) and polydimethylsiloxane (PDMS, Rhodia). The polyisoprene is nearly monodisperse with a high 1,4-*cis* content, whereas the PDMS is polydisperse. Both polymers are essentially Newtonian liquids at room temperature. The mismatch between the component viscosities may significantly affect the morphology in 50/50 blends, yet in this paper we are restricted to blends with ~30% PDMS, and a droplet-matrix morphology was always observed. Two blends are studied in this paper.

Diblock blend: The first blend, which serves as a reference, uses a PI-PDMS diblock copolymer (see Table I) as a compatibilizer. This diblock copolymer was made by sequential anionic polymerization and is nearly symmetric and monodisperse. This same compatibilizer was used by Van Hemelrijck *et al.* (2005). The diblock blend contained 1.5 wt % of the diblock copolymer, with the remainder being PDMS and PI in a 30:70 ratio.

Reactive blend: The chief concern of this paper is the second blend, dubbed the “reactive blend” in which a compatibilizer is generated by an interfacial chemical reaction between polyisoprene-graft-maleic anhydride (PIMA) and poly(aminopropylmethylsiloxane-co-dimethylsiloxane) (PDMS-NH₂). The PIMA has an (isoprene):(isoprene maleic anhydride) ratio of 98.5:1.5, and a molecular weight of 25 kg/mol; this corresponds to an average of ~4.7 anhydride groups per chain. The PDMS-NH₂ is quoted as having a molecular weight of 5 kg/mol and 2%–3% of aminopropyl groups pendant from the chain; this corresponds to an average of 1.3–1.9 amine groups per chain. A more detailed chemical characterization of both reactive species will be published in the future.

One goal of this paper is to directly image the reactively formed copolymer at the interface by confocal microscopy. This necessitates tagging one of the reactive blocks by a fluorophore. For this purpose, we used 4-chloro-7-nitrobenzofurazan (commonly known as NBD chloride). While NBD chloride is itself not fluorescent, upon reacting with an amine, it forms a fluorescent species [Fager *et al.* (1973)]. In the present case, some of the amine groups of PDMS-NH₂ were reacted with NBD chloride in a mutual solvent, dichloromethane, at room temperature. This reaction resulted in fluorescently

tagged, amino-functional PDMS, which is dubbed * PDMS-NH₂ where the “*” refers to the fluorescent tagging. For reference purposes, we also reacted the PDMS-NH₂ with excess NBD chloride, leading to complete fluorescent tagging (i.e., no unreacted amine groups). This fully tagged PDMS is dubbed * PDMS. The fluorescence emission spectra of * PDMS-NH₂ and * PDMS were recorded. The absorption spectrum of the fluorophore has a maximum at a wavelength of \sim 460 nm, whereas the peak fluorescence emission occurs at \sim 520 nm. The peak fluorescence emission intensity of * PDMS-NH₂ was found to be roughly half of that of * PDMS, suggesting that half of the original NH₂ groups of PDMS-NH₂ were reacted with NBD chloride. Accordingly, * PDMS-NH₂ has an average of 0.65–0.95 groups per chain available for reacting with PIMA.

The Introduction mentioned that the chief concern of this paper is to examine the effect of multifunctional reactive compatibilizers. From that point of view, the average functionality of the * PDMS-NH₂ appears to be too low to be “multifunctional.” Nevertheless, since a distribution of chain lengths and functionalities are expected, at least some of the * PDMS-NH₂ chains are expected to have at least two reactive groups and be capable of crosslinking, whereas those with only one reactive group would become dangling chains and not contribute to the crosslinked network. To confirm that the functionality was adequate for crosslinking, we prepared a blend of PIMA and * PDMS-NH₂ in a 1:1 weight ratio. The result was a solid mass that would not dissolve in cyclohexane, which is a good solvent for both PIMA as well as * PDMS-NH₂, suggesting that crosslinking did occur. Moreover, as the following section shows, there are profound differences between the behavior of the reactive blend and the diblock blend which are consistent with interfacial crosslinking.

The reactive blend contained 0.75 wt % of the PIMA and 0.75 wt % of the * PDMS-NH₂, and the PDMS and PI phases were in a 30:70 ratio. The total compatibilizer loading of 1.5 wt % is identical to that of the diblock blend. Moreover, assuming that the concentration of reactive groups quoted by the manufacturers is correct, and because half of the amine groups are fluorescently tagged, the two reactive species are stoichiometrically balanced, i.e., in the reactive blend, the number of anhydride groups of PIMA are equal to the number of amine groups of * PDMS-NH₂.

Blend preparation: In a recent paper [Martin and Velankar (2008)] we showed that the blending protocol can be used to significantly vary the morphology of the immiscible polymer blends, especially when a diblock compatibilizer is added. Hence, it is important to specify the blending protocol exactly. In case of the diblock blend, the two homopolymers and the diblock copolymer were all weighed into a petridish, blended with a spatula by hand, and degassed in vacuum prior to experiments. The same protocol was followed for the reactive blends, but care was taken that the reactive species did not come into contact with each other during weighing.

Methods: Bright field microscopy was performed using an Olympus CKX41 inverted microscope equipped with a Basler area scan camera. Confocal microscopy was performed using an Olympus FluoView FV1000 inverted confocal microscope using an Ar-ion laser at an excitation wavelength of 488 nm. Low magnification photographs of the samples were taken using a Canon Rebel XT digital camera. Rheological experiments were performed using a TA Instruments AR2000 stress-controlled rheometer with 40 mm/1° cone and plate geometry, and the sample temperature of 25 °C was maintained using a Peltier cell.

III. RESULTS

A. Morphology

Immediately after blending, a drop of each blend was placed between glass slides separated by a thin spacer and examined by optical microscopy. Figure 2(a) shows that the diblock blend exhibits a typical drop matrix morphology composed of round drops of diameter on the order of several microns. The PI, which is the majority phase, is expected to become the continuous phase. This was verified by placing a drop of the blend, and a drop of pure PI, next to each other on a slide. As the two drops spread and touched each other, no interface was evident, confirming that PI is the continuous phase of the diblock blend.

The reactive blend was also found to have a PI-continuous morphology. Optical microscopy of the reactive blend is slightly more difficult since it does not flow readily (see below) and hence tended to form a thick "lump" on the microscope slide (in contrast the diblock blend spread into a relatively thin film). The large sample thickness, combined with the intense scattering, did not permit good images. By squeezing the reactive blend between slides, it was forced into a thin film and the corresponding image, Fig. 2(b), shows that the corresponding morphology is somewhat different from that of the diblock blend, specifically, the drops appear to be clustered together. Close observation also suggests that some drops are nonspherical, whereas some appear fused with their neighbors. The morphology of Fig. 2(b) may be affected by the fact that the sample was squeezed between slides. It is therefore desirable to image the morphology without the excessive squeezing flow. In order to realize a thin film without excessive squeezing, a small sample of the reactive blend was placed on a slide, and covered with a few drops of light mineral oil, which can dissolve the matrix phase PI. After several hours, the matrix phase PI dissolved in the mineral oil causing the blend to spread in a thin layer on the slide, and greatly improving the quality of the image. (Note that the mineral oil also has some solubility in the PDMS and the drops are likely to be somewhat swollen by the oil.) The cluster structure became clearly apparent [Fig. 2(c)] in this oil-treated sample, in fact, many drops appear to be connected to form a network. Furthermore, close observation reveals that some of the drops may not have smooth surfaces, as illustrated in the magnified view of a portion of Fig. 2(c). We attribute all three features (nonspherical drops, their nonsmooth surface, and the network of drops) to the multifunctional nature of the reactive species. Specifically, we propose that the interface of each drop is a soft solid shell or "skin" of crosslinked compatibilizer. It is this solid-like nature of the interface that is responsible for the occasional nonspherical drops and the nonsmooth interfaces.

Since the reactive PDMS is fluorescently tagged, the compatibilizer can be imaged directly by fluorescence microscopy. Figure 2(d) shows a confocal microscope image of the blend. Since this image was taken on an "as-prepared" blend [i.e., without oil treatment of Fig. 2(c)] it is truly representative of the morphology of the blends. The drops in Fig. 2(d) appear to be covered by bright shells of compatibilizer, with relatively little fluorescence evident inside the bulk of the drops. In contrast, Fig. 2(e), which is a similar blend but without PIMA added to the PI phase shows uniformly bright drops indicating that the * PDMS-NH₂ is evenly distributed throughout the bulk. Thus, the bright shells of Fig. 2(d) are evidence that the reactive * PDMS-NH₂ is present at the interface, and that such interfacial localization is definitely attributable to the reaction with the anhydride. Furthermore, Fig. 2(d) confirms that the drops are clustered together. At the end of this paper we will propose a possible reason for the clustering. Finally, in agreement with Fig. 2(c), some drops appear to be somewhat nonspherical, although grossly distorted shapes are not evident.

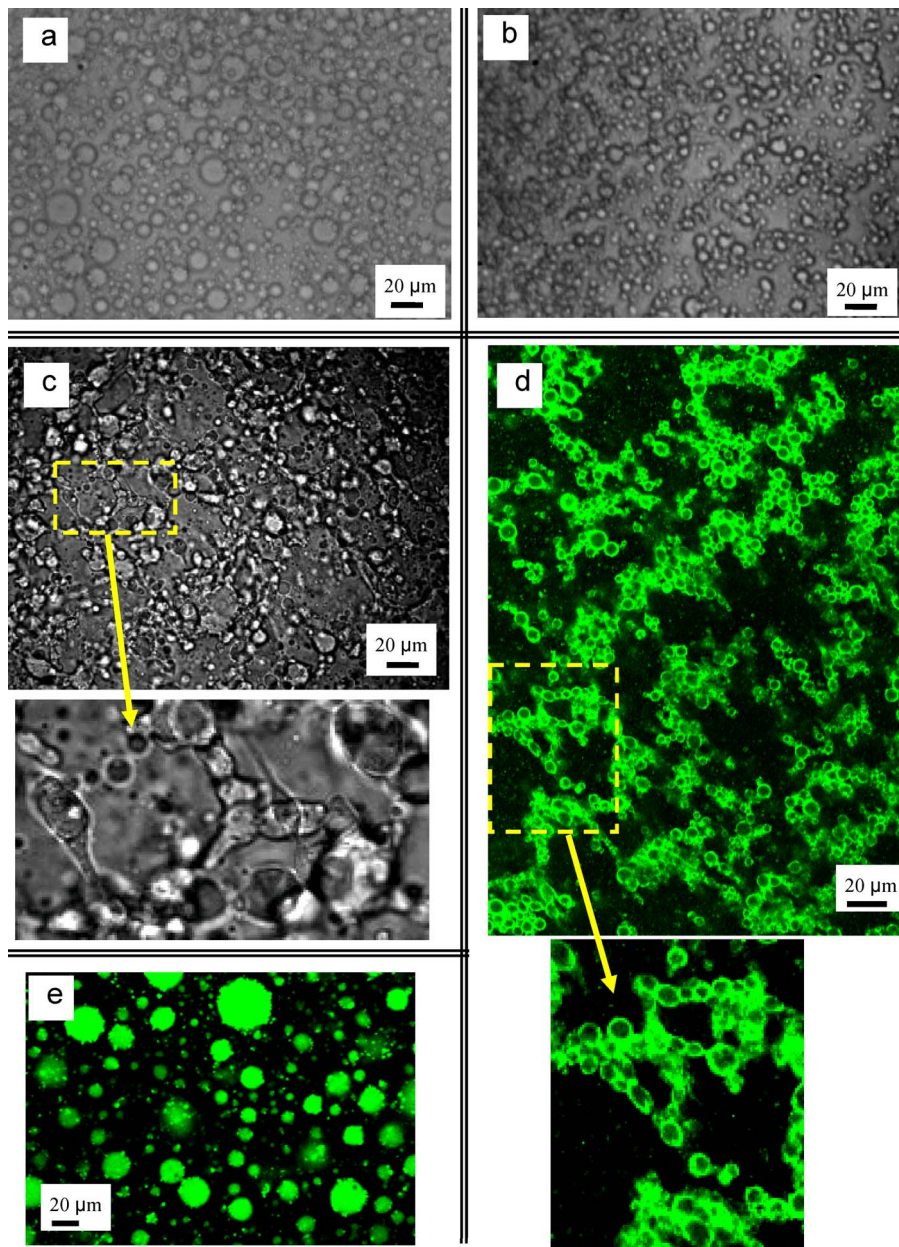


FIG. 2. Microscopic images of: (a) bright field diblock blend, (b) bright field reactive blend, (c) reactive blend after diluting with mineral oil, with the dotted rectangle being shown in magnified form as indicated by the arrow, and (d) confocal image of reactive blend, with the dotted rectangle being shown in magnified form as indicated by the arrow. (e) confocal image of the reactive blend, but without PIMA. Images (d) and (e) are colored in the electronic version.

The remainder of this paper explores the rheology of the reactive blends. Before proceeding with the quantitative investigation of the rheology, it is worth noting a qualitative rheological difference between the reactive and the diblock blends that is evident even from simple visual observation. During blending, numerous air bubbles were en-

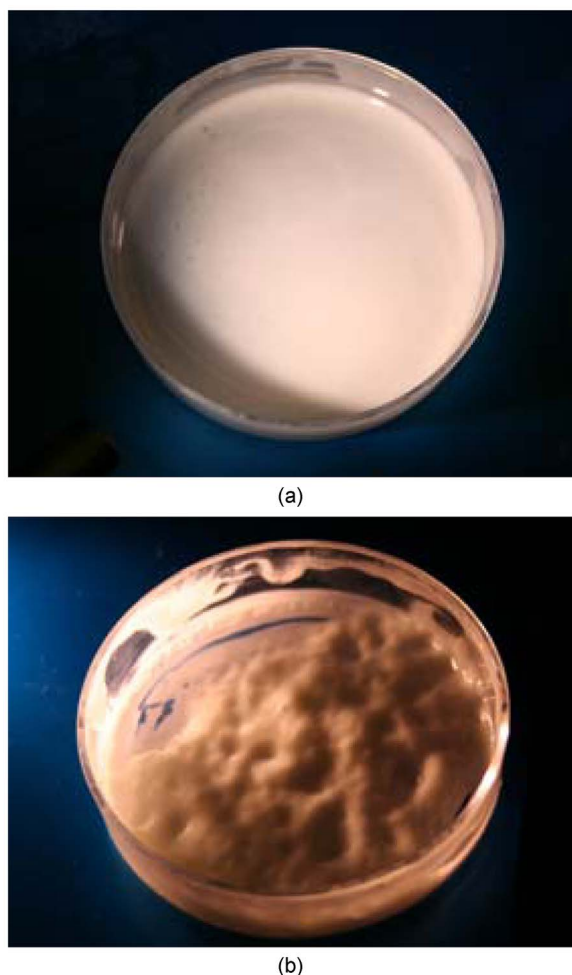


FIG. 3. Macroscopic image of (a) diblock blend (b) and reactive blend. (Images are in color in the online version.)

trained within both blends, and these were removed by degassing in vacuum at room temperature. At the end of the degassing process, the diblock blend settled in a uniform, thick layer in the petridish [Fig. 3(a)]. In contrast, after degassing, the reactive blend showed an irregular surface [Fig. 3(b)] with some portions of the sample being much thicker than others. The bumpiness at the surface of the reactive blend in the petridish relaxed with time, but even after 20 h, it still did not flatten out. These visual observations suggest that the reactive blend is highly viscous, or perhaps has a small yield stress—possibilities that are supported by the more quantitative measurements of the following section.

B. Rheology: Dynamic oscillatory properties of as-prepared blends

Strain-sweep measurements were conducted at four different frequencies (100, 10, 1, and 0.1 rad/s) for strains ranging from 0.1% to 10%. Both blends showed linear dynamic mechanical properties under these conditions. All subsequent oscillatory measurements were conducted at 1% strain.

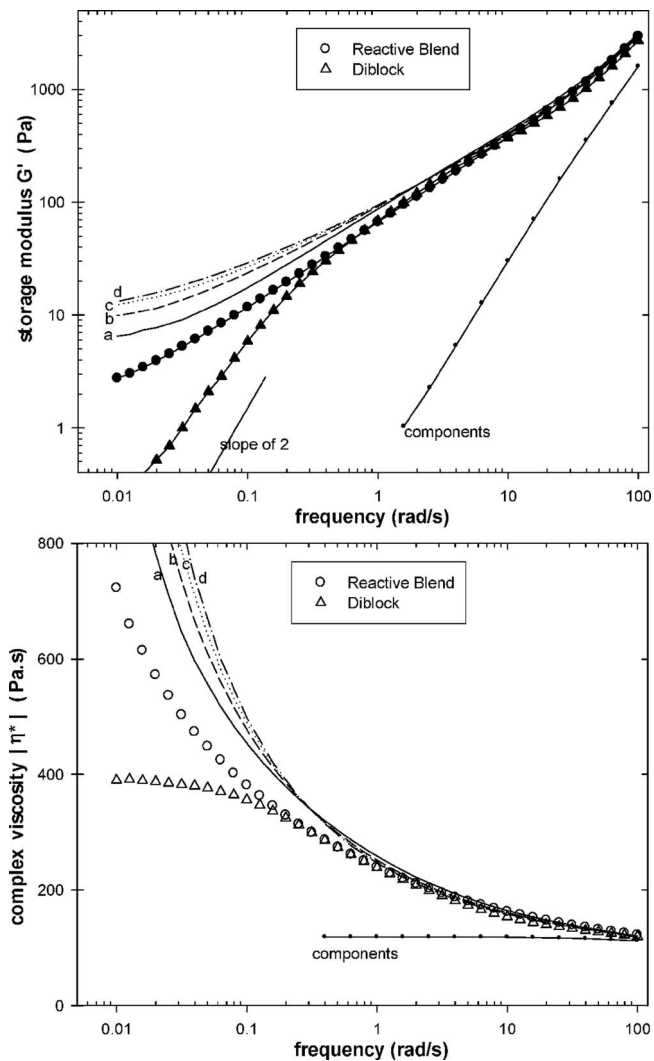


FIG. 4. Dynamic oscillatory properties of the diblock blend and reactive blend as loaded into the rheometer. Open symbols refer to the complex viscosity and closed symbols refer to the storage modulus. The lines labeled (a)–(d) are four successive frequency sweeps for the reactive blend. The data labeled “components” are a volume-weighted average of the bulk PI and PDMS.

Figure 4 compares the dynamic oscillatory frequency sweep behavior of both blends at 1% strain. The behavior of the diblock blend is similar to similar blends studied previously [Velankar *et al.* (2001); Van Hemelrijck *et al.* (2004); Wang and Velankar (2006); Martin and Velankar (2007)]. In particular, the diblock blend shows a higher G' and a higher $|\eta^*|$ as compared to the pure components at low frequencies. This indicates that the diblock blend has additional relaxation processes that are absent in the components. These additional relaxations have been attributed to the shape-relaxation of drops of the blend [Oldroyd (1953); Paliarne (1990); Graebling *et al.* (1993)], and to the interfacial viscoelasticity of the compatibilizer [Oldroyd (1955); Riemann *et al.* (1997); Jacobs *et al.* (1999); Van Hemelrijck *et al.* (2004)]. At low frequencies, the diblock blend has a G' that is nearly proportional to the square of the frequency, and the $|\eta^*|$ shows a plateau—both characteristics of the terminal behavior of a viscoelastic liquid.

Turning to the reactive blend, the high-frequency oscillatory properties of this blend appear to be similar to those of the diblock blend. However, at low frequencies in the reactive blend, the G' decreases much less steeply than ω^2 , whereas the complex viscosity increases with no sign of leveling off to some well-defined terminal value. Such behavior is termed as “gel-like” behavior in this paper. Such gel-like behavior, which suggests that the blend has an extremely high terminal viscosity (or a yield stress), is a quantitative explanation for why the degassed blend did not relax in the petridish in Fig. 3(b).

The properties of the diblock blend under quiescent conditions did not change with time over the timescale of the oscillatory test; repeated oscillatory measurements gave identical results. In contrast, repeated oscillatory tests on the reactive blend showed significant changes in the rheological properties with time even under quiescent conditions. For example, Fig. 4 shows that the G' and the $|\eta^*|$ of the reactive blend in the low frequency region increased sharply after just one frequency sweep lasting about 100 min [curve (a)] with further small increases over three additional frequency sweeps lasting an additional 5 h [curves (b),(c),(d)]. The reason for these changes is not clear. It may be that the deformation experienced by the sample during loading relaxes over a long timescale, and the corresponding changes in morphology enhance the gel-like behavior. It is also possible that the drops aggregate into clusters under quiescent conditions, and later in the paper we will present rheological data that support this drop aggregation hypothesis.

A common concern when dealing with multifunctional reactive systems is the possibility that the entire bulk may become crosslinked, rendering the material virtually unprocessable, similar to a thermoset [Baker *et al.* (2001b)]. In the present case, only 3% of the entire system has reactive functionality, furthermore, the crosslinking is confined to the interface. Accordingly, crosslinking of the entire bulk seems unlikely. Nevertheless, since the dynamic oscillatory properties indicate gel-like behavior, the issue of processibility must be considered in more detail. We therefore address two issues in the following two sections: (1) rheological behavior upon startup of steady shearing which is an indicator of flow-induced breakdown of the gel-like behavior, and (2) rheological behavior (especially viscosity) under steady shearing, which is the most basic indicator of processibility.

C. Rheology: Startup of shearing

The shear history used to investigate structural breakdown is illustrated in Fig. 5(a). It consisted of a series of successively longer shearing steps (creep steps) ranging from 20 s to 15 min, all at a fixed stress of 100 Pa (chosen arbitrarily). The strain recovery upon cessation of shear, i.e., the recovery at the end of each creep step, was monitored.

For the diblock blend, in each creep step, the viscosity (formally denoted η_c^+) shows a weak overshoot [Fig. 5(b)], with the steady shear viscosity being reached in less than 10 s. Upon cessation of shear [Fig. 5(d)], the recovery is completed in about 10 s. All creep steps show identical behavior, and all recovery steps also show identical behavior, both of which indicate that shearing at 100 Pa causes no morphological changes in this sample. Typically, two morphological changes are possible: flow-induced drop breakup, or flow-induced coalescence. Flow-induced coalescence is not expected in the present case because the PI-*b*-PDMS diblock copolymer is known to suppress coalescence of PDMS drops in PI [Van Hemelrijck *et al.* (2005)]. Drop breakup is not expected either because the hand-blending process involves high stresses (likely much higher than 100 Pa), and hence, the drop size of the as-prepared blend is already expected to be

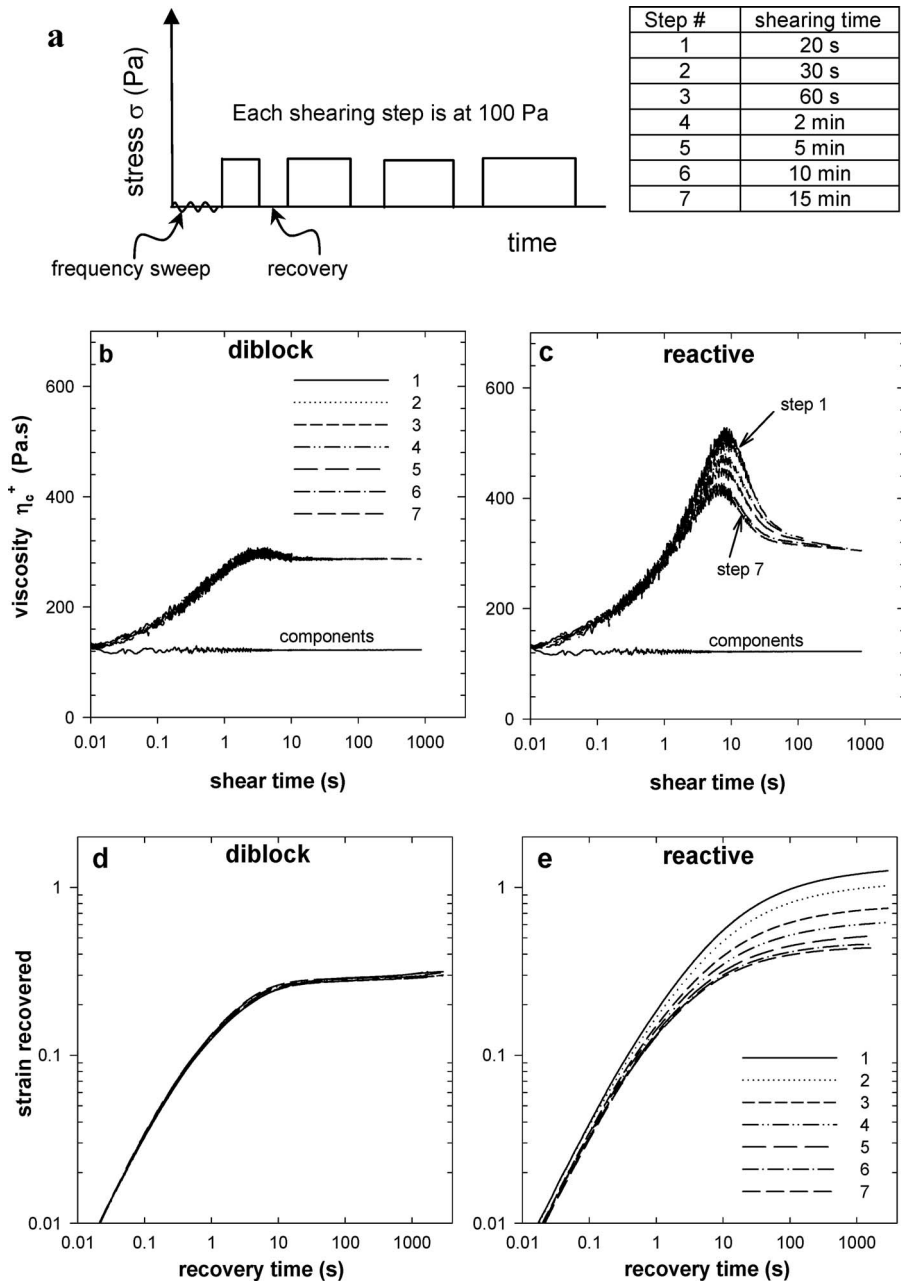


FIG. 5. (a) Shear history. The table shows the shearing time in each step. (b),(c) viscosity during each shearing step listed in the legend. (d), (e) recovery upon cessation of shear after each shearing step listed in the legend. In (c), the highest peak is shown by step 1, and each successive step shows a weaker peak. The data labeled components in (b) and (c) are volume-weighted averages of the bulk PI and PDMS.

smaller than the critical drop size at 100 Pa. Since neither coalescence nor breakup are expected, consistent behavior of the sample during or after each 100 Pa shearing step is not surprising.

Next we will consider the behavior of the reactive blend. The most important quali-

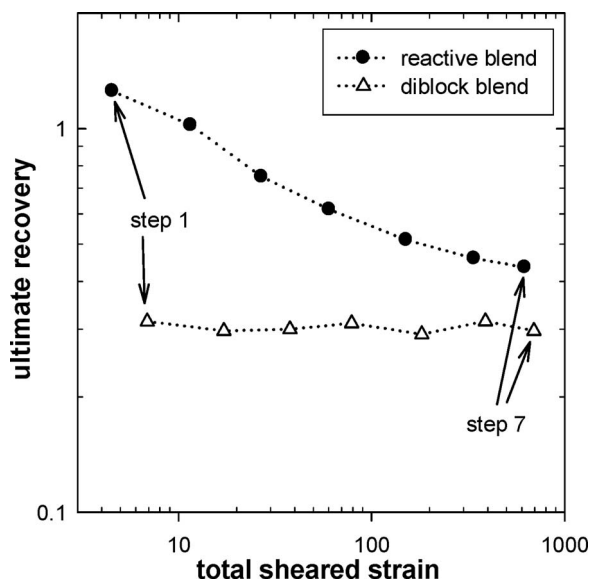


FIG. 6. Ultimate recovery, γ_{∞} , as a function of total sheared strain for both blends. The recovery vs time data for the reactive blend had not fully leveled off, thus, the actual γ_{∞} for the reactive blend is slightly higher than shown here.

tative change evident from the creep steps is a large overshoot in the viscosity η_c^+ of the sample [Fig. 5(c)] at short shearing times. The magnitude of the overshoot is largest during the first shearing step and decreases in subsequent steps, yet it is noteworthy that the overshoot persists even after shearing for several hundred seconds (corresponding to several hundred strain units). The recovery behavior of the reactive blend [Fig. 5(e)] also differs qualitatively and quantitatively from the diblock blend. First, the recovery kinetics are much slower; an unambiguous plateauing of the strain vs time data (indicating the ultimate recovery of the sample) is not reached even after 1000 s, especially in the early shearing steps. Second, the magnitude of the ultimate recovery is much larger than for the diblock blend. This becomes clearer when the ultimate recovery is plotted as a function of the total strain experienced by the sample (Fig. 6); for the early steps, the ultimate recovery of the reactive blend is more than double that of the diblock blend.

D. Rheology: Steady shear characteristics

At the conclusion of the rheological test of the previous section, the samples were subjected to the shear history of Fig. 7(a). The sample was sheared at 400 Pa for 2000 strain units, then the subsequent recovery upon cessation of shear was monitored, followed by an oscillatory frequency sweep at 1% strain. This sequence (shear for 2000 strain units, recovery, and oscillatory) was repeated at five successively lower stresses of 400, 200, 100, 50, and 25 Pa.

The rheological behavior of the diblock blend [Figs. 7(b), 7(d), and 7(f)] resembles data on similar samples measured previously. Note that Fig. 7(f) shows only one set of data for the diblock, viz. the G' and the $|\eta^*|$ recorded after shearing at the 400 Pa stress level. Data after shearing at lower stress levels (not shown) are almost identical to this curve, furthermore, the “as loaded” data for the diblock (Fig. 4) are also identical to this

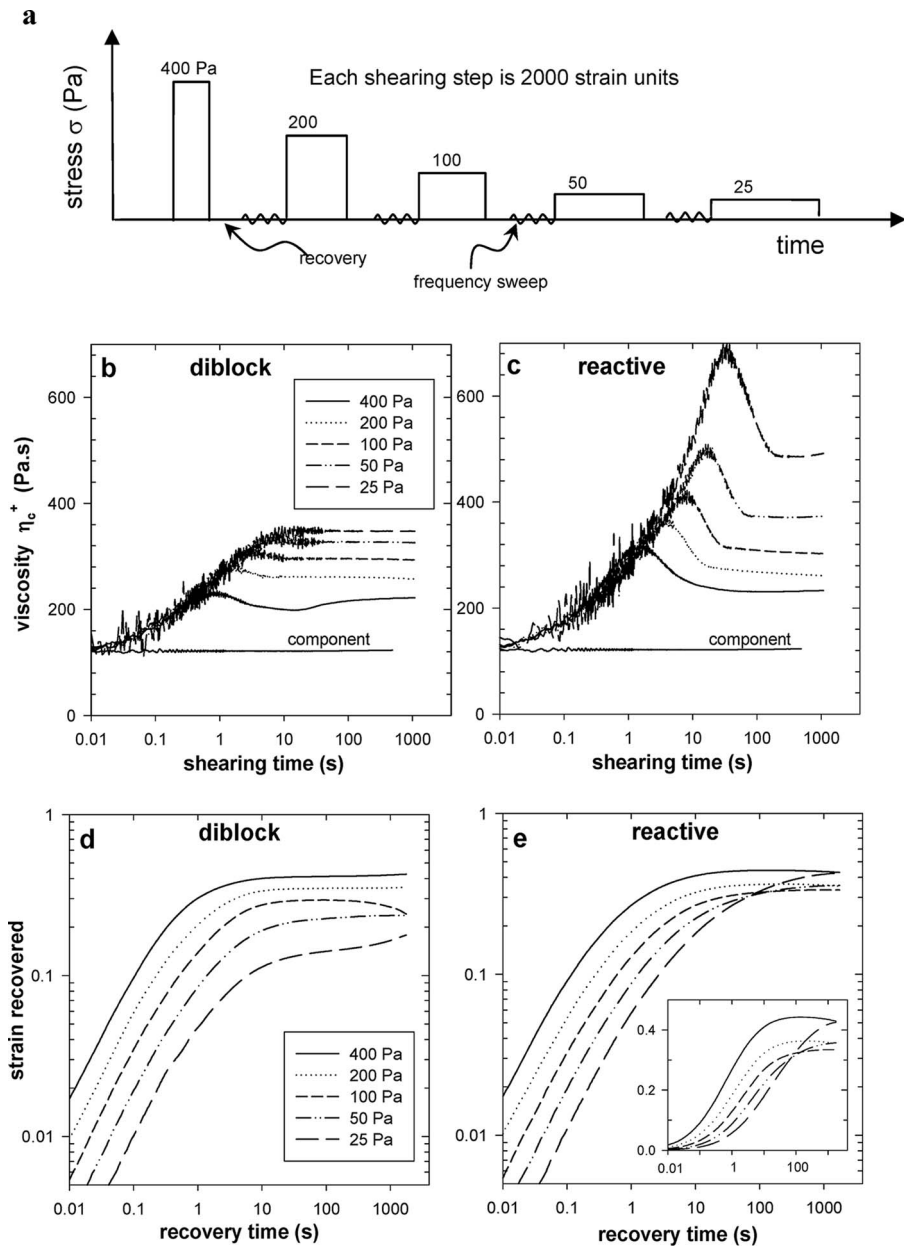


FIG. 7. (a) Shear history. Note that the samples experienced the shear history of Fig. 5 (a) prior to this experiment. (b), (d) Data for diblock blend. (c), (e) Data for reactive blend. (b), (c) Startup of creep at the various stresses listed in the legend. (d), (e) Recovery upon cessation of shear following the various stresses listed in the legend. The inset in (e) shows the same data on a linear y-scale. (f) Oscillatory behavior of both blends subsequent to shearing at the stresses listed in the legend. Diblock data are shown only at 400 Pa since data at all lower stresses nearly superpose upon the 400 Pa curves. The data labeled components in (b), (c), and (f) are volume-weighted averages of the bulk PI and PDMS.

curve. All the observed trends can be interpreted by simply recognizing that since coalescence is suppressed, shearing at successively lower stresses does not affect the drop size. Accordingly, (1) the oscillatory properties, which are expected to depend only on

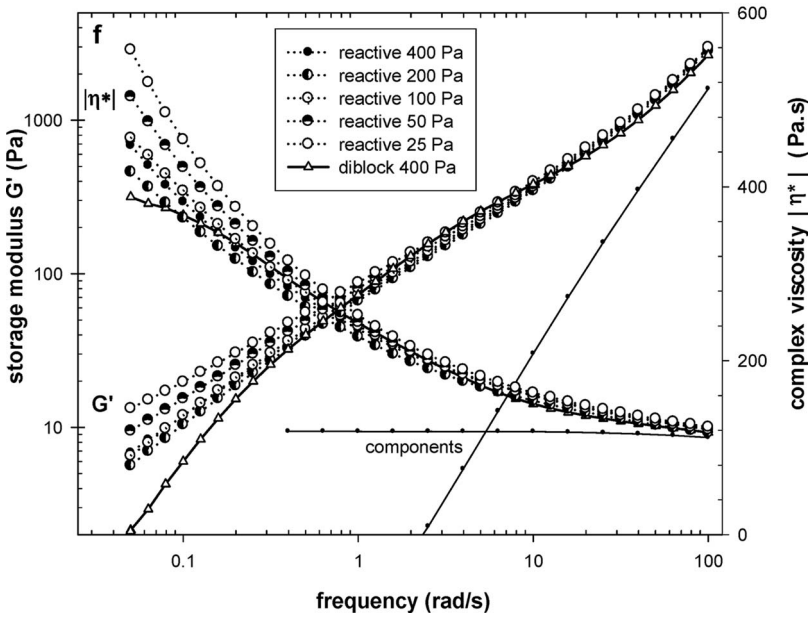


FIG. 7. (Continued).

drop size, are unaffected by shearing at various stresses, (2) the transient time during startup of creep [Fig. 7(b)] which is expected to scale with (drop size)/stress increases with decreasing stress, (3) the magnitude of the ultimate recovery [Fig. 7(d)], which is expected to scale with stress/(drop size), decreases with decreasing stress, and (4) decreasing stress without changing the drop size reduces the capillary number, thus explaining the observed shear thinning [Fig. 7(b)].

The rheological behavior of the reactive blend in the same experiment shows several differences. Similar to the data of Fig. 5(c), the viscosity η_c^+ of the reactive blend [Fig. 7(c)] during the creep steps shows a peak before reducing again to a steady shear value. The peak magnitude as well as the steady shear viscosity both increase with decreasing stress. The recovery behavior of the reactive blend [Fig. 7(e)] is qualitatively similar to that of the diblock blend at high stress levels. However, at the lowest two stress levels, the ultimate recovery increases again. This is more clearly evident in the inset to Fig. 7(e); the linear y-scale highlights the sharp increase in ultimate recovery after the 25 Pa shearing step. Finally, Fig. 7(f) shows the evolution of the dynamic moduli after shearing the sample. It is clear that shearing does not destroy the gel-like behavior; indeed, at the lowest two stress levels, shearing significantly enhances the gel-like behavior as evidenced from the larger magnitude of the G' and the larger upturn in $|\eta^*|$ at low frequencies.

Figure 8 plots some of the key features of Fig. 7 quantitatively. The location of the maximum in the η_c^+ vs. time data is seen to scale nearly inversely with the stress [Fig. 8(a)]. The peak magnitude increases with decreasing stress [Fig. 8(b)], but no simple relationship between the peak magnitude and the stress is apparent from the data. We have also examined two related quantities: the interfacial contribution to the peak magnitude [defined as (peak magnitude)—(volume-averaged viscosity of the components)], and the excess viscosity [defined as (peak magnitude)—(steady shear viscosity)]. Neither of these quantities shows any simple dependence on stress. Figure 8(c) compares the

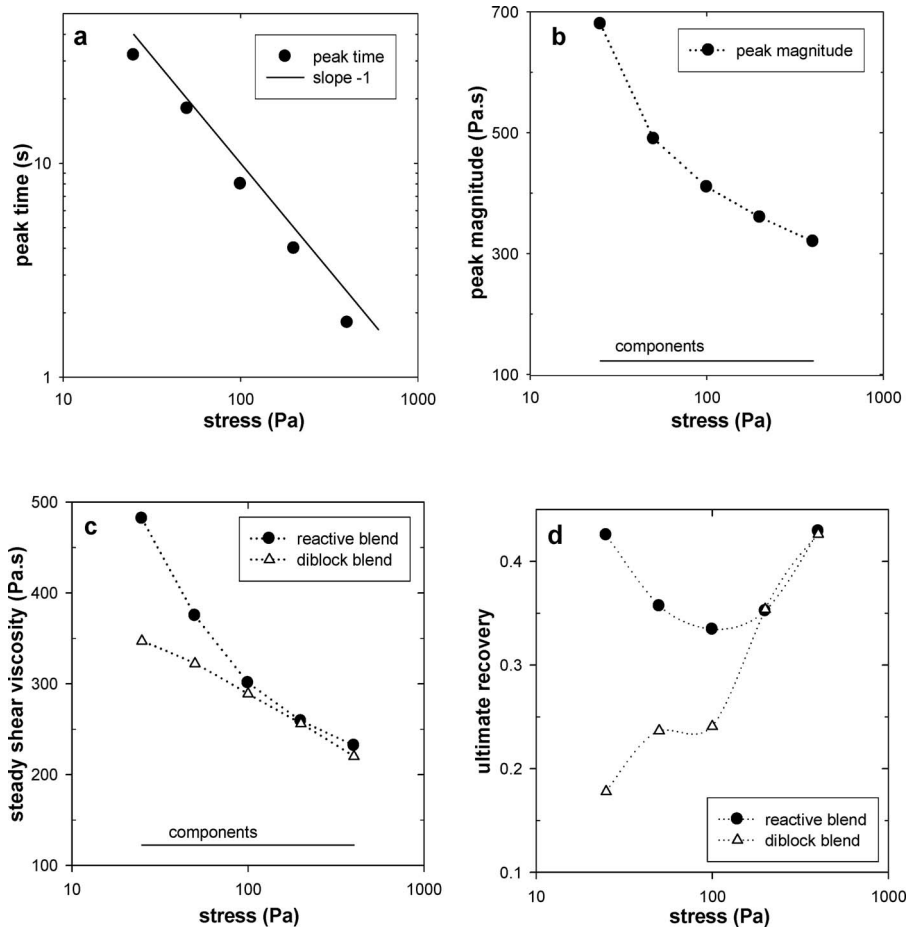


FIG. 8. (a) Position and (b) magnitude of the viscosity overshoot of the reactive blend shown in Fig. 7(e). (c) Steady shear viscosity recorded at long shearing times in Figs. 7(b) and 7(e). (d) Ultimate recovery from Figs. 7(c) and 7(f). The line labeled components in (b) and (c) is a volume-weighted average of the bulk PI and PDMS.

steady shear viscosities of the two blends. The viscosity of the two blends is comparable at high stress, but below 100 Pa, the reactive blend has a sharply higher viscosity, with no sign of leveling off to a zero-shear plateau. Finally, the ultimate recovery for the two blends is compared in Fig. 8(d). As with the viscosity, the ultimate recovery is very similar for the two blends at high stresses, however, upon decreasing stress, the reactive blend shows a sharp increase in recovery.

E. Summary and discussion

We first review the chief observations about the reactive blend.

- (1) Optical and confocal microscopy reveal three unusual features about the reactive blend: that some drops are nonspherical, that they are connected together in clusters, and that some drops have interfaces that do not appear smooth. Confocal microscopy also shows fluorescent shells around the drops, confirming that the reaction between *PDMS-NH₂ and PIMA has indeed occurred.

- (2) Rheologically, the reactive blend shows gel-like behavior at low frequencies in dynamic oscillatory experiments. With decreasing stress, the steady shear viscosity and strain recovery after cessation of shear increase sharply. Finally, the creep behavior shows a large peak in the viscosity at short shearing times, especially at low stress.
- (3) The gel-like behavior in dynamic oscillatory experiments and the peak in viscosity in creep experiments both persist even after shearing the sample for several hundred strain units.

To our knowledge, similar features have been noted previously in only one reactive blend. [Sailer and Handge \(2007\)](#) examined the morphology and rheology of blends of polyamide and maleated styrene-acrylonitrile (SAN) with of ~ 20 maleic anhydride groups per chain. They noted drop clusters, a large increase in elastic recovery, and nonliquid-like dynamic mechanical behavior in the reactively compatibilized blends. They attributed these observations to “elastic interactions between grafted shells,” but the mechanism for the elastic interactions is not clear. It is possible that the much higher amount of graft copolymer possible in that system (since their maleated SAN chains had a high functionality and all the PA6 was reactive) is responsible for their unusual rheology.

Two issues bear further discussion. The first is the structural origin of the gel-like oscillatory behavior [Figs. 4 and 7(f)] and the peak in the viscosity at short shearing times [Figs. 5(c) and 7(c)]. The fact that the gel-like behavior and the viscosity overshoot persist and even grow stronger upon shearing suggest that it is a physical network (rather than a network of chemical crosslinks) that is responsible for these rheological features. We hypothesize that the physical network is comprised of large drop clusters, and that under low stress shearing, the clusters can grow to a relatively large size, causing enhanced gel-like behavior and larger ultimate recovery. One may also expect clusters to grow under quiescent conditions, and this suggests the following possible mechanism to explain the viscosity overshoot upon startup of shear of Fig. 7(c): Each creep step is preceded by a half hour strain recovery step and a ~ 1 h oscillatory step. If clusters grow under these nearly quiescent conditions, the subsequent breakdown of these clusters may be responsible for the viscosity overshoots. To test this, we directly examined whether the viscosity overshoot grows with “rest time” after cessation of shearing. The reactive blend was subjected to the shear sequence of Fig. 9(a), where the blend was sheared repeatedly at 100 Pa for 500 strain units, with an increasing rest time between successive shearing steps. Indeed Figs. 9(b) and 9(c) show that the viscosity overshoot increases steadily with rest time. These data support the idea that the viscosity overshoots are caused by physical changes in the blend structure during quiescent conditions. Whether these physical changes do indeed correspond to droplet clustering as hypothesized above is presently being tested by direct visualization. What is the mechanism for the droplets to form clusters? We speculate that clusters occur because the drops attract each other due to van der Waals forces. These would ordinarily lead to coalescence, however, in the present case, the crosslinked skin is able to prevent coalescence, and hence, the drops stick to each other forming clusters.

The second issue concerns processibility. As mentioned in Sec. III B, when dealing with crosslinkable materials, a common concern is whether the system remains processible. Figure 8 allays this concern: at high stress levels typical of polymer processing, the viscosity as well as the creep recovery of the reactive blend is quite similar to that of the diblock blend. It is only at stresses lower than 100 Pa that the rheology of the reactive

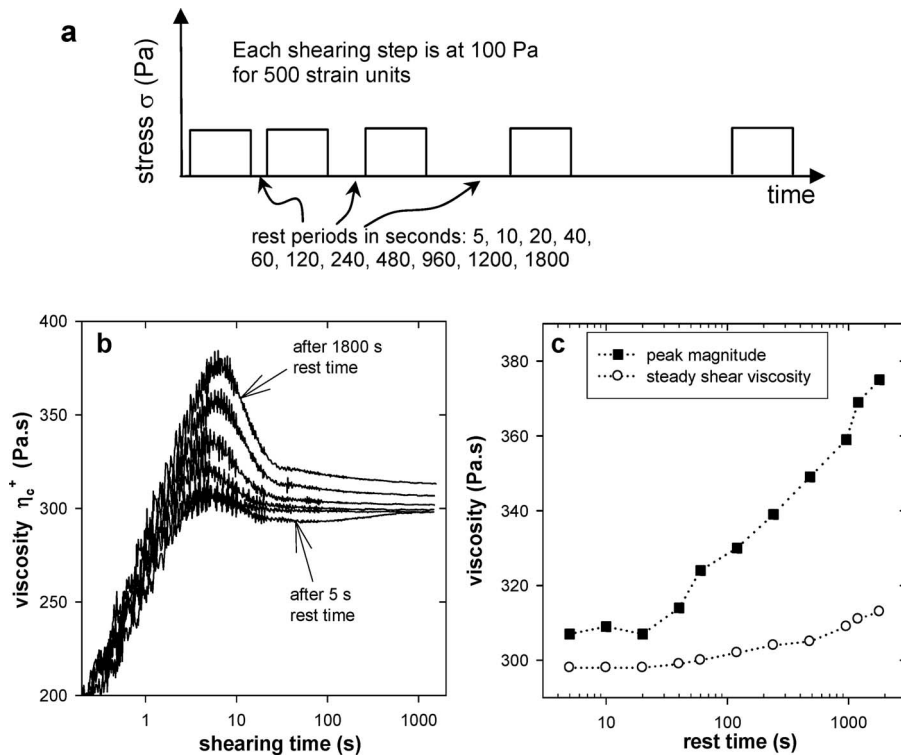


FIG. 9. (a) Shear protocol for testing effect of rest period on viscosity overshoot. (b) Startup of creep at 100 Pa after each rest time. Only some steps are shown for clarity. (c) Magnitude of viscosity overshoot as a function of rest period. Closed squares are the peak viscosity; open circles are the viscosity at the end of the step (i.e., at 500 strain units). The vertical distance between the two symbols is the viscosity overshoot.

blend departs qualitatively from that of the diblock blend. Thus, we tentatively conclude that using multifunctional compatibilizers to crosslink interfaces does not adversely affect the processibility of the blends.

IV. CONCLUSIONS

We have examined the effect of reactive compatibilization using two multifunctional species in model blends of PI and PDMS. The blends consisted of PDMS and PI in a 30:70 ratio, along with a total of 1.5% of multifunctional reactive PI and PDMS for compatibilization. Optical microscopy shows significant differences between the morphology of the reactive blend and a reference blend compatibilized by a diblock copolymer. The diblock blend shows a “normal” droplet-matrix morphology. In contrast, the reactive blend was characterized by nonspherical drops, drop clustering, and some non-smooth drop surfaces. We believe that the multifunctional reactive compatibilizer forms a crosslinked skin on the surface of the drops. Such an interface is a soft solid which cannot be characterized simply by an interfacial tension. It is the solid-like nature of the interface that permits nonspherical drop shapes to persist. We hypothesize that drops cluster together because they attract each other by van der Waals forces, but cannot coalesce due to their crosslinked skin.

The rheological properties of the diblock blend resemble those of similar systems studied previously and are consistent with the previous observation that the diblock

compatibilizer suppresses coalescence. In contrast, the reactive blend shows many unusual rheological features including a high viscosity and high creep recovery at low stress, overshoots in viscosity in creep experiments, and gel-like oscillatory behavior. Nevertheless, at high stress levels, the rheological properties of the reactive blend are nearly identical to those of the diblock blend, i.e., multifunctional reactive compatibilization, at least at 1.5% of compatibilizer, does not significantly affect the processibility.

Finally, we note that a crosslinked interfacial skin offers new opportunities for controlling the morphology of immiscible polymer blends. In particular, the fact that the crosslinked interface can resist capillary pressure due to interfacial tension may prove useful in stabilizing anisotropic morphologies. This will be studied in future research.

ACKNOWLEDGMENTS

The authors are grateful to the Laboratory of Applied Rheology at the Katholieke Universiteit Leuven for making the PI-PMDS diblock copolymer available for this research. The authors thank Rhodia Silicones and Kuraray Co. for providing the PDMS and PI homopolymers, respectively, the Center for Biological Imaging at the University of Pittsburgh for use of their microscopy facilities, and Dr. Toby Chapman, University of Pittsburgh, for his advice regarding fluorescent labeling. This research was supported by CAREER Grant No. CBET-0448845 and IGERT Grant No. DGE-0504345 from the National Science Foundation, and by the Mascaro Sustainability Initiative at the University of Pittsburgh.

References

- Aycock, D. F., and S.-P. Ting, "Polyphenylene ether-polyamide blends," US Patent No. 4,600,741 (1986).
- Aycock, D. F., and S.-P. Ting, "Acyl modified polyphenylene ether composition," US Patent No. 4,642,358 (1987).
- Baker, W., C. Scott, and G. H. Hu, *Reactive Polymer Blending* (Hanser Gardner, Cincinnati, 2001a), Chaps. 4 and 5.
- Baker, W., C. Scott, and G. H. Hu, *Reactive Polymer Blending* (Hanser Gardner, Cincinnati, 2001b), Sec. 4.3.
- Beck Tan, N. C., D. G. Peiffer, and R. M. Briber, "Reactive reinforcement of polystyrene/poly(2-vinylpyridine) interfaces," *Macromolecules* **29**, 4969–4975 (1996).
- Beretta, C., and R. A. Weiss, "Miscibility enhancement of polymer blends by interacting functional groups," *Polym. Mater. Sci. Eng.* **56**, 556–559 (1987).
- Brown, S. B., D. J. McFay, I. Yates, B. John, and G. F. Lee, "Solvent-resistant, compatible blends of polyphenylene ethers and thermoplastic polyesters," US Patent No. 5,079,297 (1992).
- Cernohous, J. J., C. W. Macosko, and T. R. Hoyer, "Anionic synthesis of polymers functionalized with a terminal anhydride group," *Macromolecules* **30**, 5213–5219 (1997).
- Chen, L. F., B. Wong, and W. E. Baker, "Melt grafting of glycidyl methacrylate onto polypropylene and reactive compatibilization of rubber toughened polypropylene," *Polym. Eng. Sci.* **36**, 1594–1607 (1996).
- Datta, S., and D. J. Lohse, *Polymeric Compatibilizers* (Hanser, Munich, 1996).
- Fager, R. S., C. B. Kutina, and E. W. Abrahamson, "Use of NBD chloride (7 chloro-4-nitrobenzo-2-oxa-1,3-diazole) in detecting amino acids and as an N-terminal reagent," *Anal. Biochem.* **53**, 290–294 (1973).
- Graebing, D., R. Muller, and J. F. Palierne, "Linear viscoelasticity of incompatible polymer blends in the melt in relation with interfacial properties," *J. Phys. IV* **3**, 1525–1534 (1993).
- Hale, W., H. Keskkula, and D. R. Paul, "Compatibilization of PBT/ABS blends by methyl methacrylate glycidyl methacrylate ethyl acrylate terpolymers," *Polymer* **40**, 365–377 (1999).
- Hu, Y. T., and A. Lips, "Estimating surfactant surface coverage and decomposing its effect on drop deformation," *Phys. Rev. Lett.* **91**, 044501 (2003).

- Hu, Y. T., D. J. Pine, and L. G. Leal, "Drop deformation, breakup, and coalescence with compatibilizer," *Phys. Fluids* **12**, 484–489 (2000).
- Jacobs, U., M. Fahländer, J. Winterhalter, and C. Friedrich, "Analysis of Palierne's emulsion model in the case of viscoelastic interfacial properties," *J. Rheol.* **43**, 1497–1509 (1999).
- Jeon, H. K., C. W. Macosko, B. Moon, T. R. Hoye, and Z. H. Yin, "Coupling reactions of end- vs mid-functional polymers," *Macromolecules* **37**, 2563–2571 (2004).
- Kim, H. Y., D. Y. Ryu, U. Jeong, D. H. Kho, and J. K. Kim, "The effect of chain architecture of *in situ* formed copolymers on interfacial morphology of reactive polymer blends," *Macromol. Rapid Commun.* **26**, 1428–1433 (2005).
- Kim, S., J. K. Kim, and C. E. Park, "Effect of molecular architecture of *in situ* reactive compatibilizer on the morphology and interfacial activity of an immiscible polyolefin/polystyrene blend," *Polymer* **38**, 1809–1815 (1997).
- Koning, C., M. Van Duin, C. Pagnoulle, and R. Jerome, "Strategies for compatibilization of polymer blends," *Prog. Polym. Sci.* **23**, 707–757 (1998).
- Lee, P. C., W. F. Kuo, and F. C. Chang, "*In-situ* compatibilization of PBT/ABS blends through reactive copolymers," *Polymer* **35**, 5641–5650 (1994).
- Lin, B., F. Mighri, M. A. Huneault, and U. Sundararaj, "Effect of premade compatibilizer and reactive polymers on polystyrene drop deformation and breakup in simple shear," *Macromolecules* **38**, 5609–5616 (2005).
- Liu, N. C., H. Q. Xie, and W. E. Baker, "Comparison of the effectiveness of different basic functional-group for the reactive compatibilization of polymer blends," *Polymer* **34**, 4680–4687 (1993).
- Majumdar, B., H. Keskkula, and D. R. Paul, "Effect of the nature of the polyamide on the properties and morphology of compatibilized nylon/acrylonitrile-butadiene-styrene blends," *Polymer* **35**, 5468–5477 (1994).
- Martin, J., and S. Velankar, "Effects of compatibilizer on immiscible polymer blends near phase inversion," *J. Rheol.* **51**, 669–692 (2007).
- Martin, J. D., and S. S. Velankar, "Varying the blending protocol to control the morphology of model compatibilized polymer blends," *AIChE J.* **54**, 791–801 (2008).
- Martin, P., J. Devaux, R. Legras, M. van Gurp, and M. van Duin, "Competitive reactions during compatibilization of blends of polybutyleneterephthalate with epoxide-containing rubber," *Polymer* **42**, 2463–2478 (2001).
- Oldroyd, J. G., "The elastic and viscous properties of emulsions and suspensions," *Proc. R. Soc. London, Ser. A* **218**, 122–132 (1953).
- Oldroyd, J. G., "The effect of interfacial stabilizing films on the elastic and viscous properties of emulsions," *Proc. R. Soc. London, Ser. A* **232**, 567–577 (1955).
- Oshinski, A. J., H. Keskkula, and D. R. Paul, "Rubber toughening of polyamides with functionalized block copolymers. 2. Nylon-6,6," *Polymer* **33**, 284–293 (1992).
- Oshinski, A. J., H. Keskkula, and D. R. Paul, "The effect of polyamide end-group configuration on morphology and toughness of blends with maleated elastomers," *J. Appl. Polym. Sci.* **61**, 623–640 (1996).
- Palierne, J. F., "Linear rheology of viscoelastic emulsions with interfacial tension," *Rheol. Acta* **29**, 204–214 (1990).
- Riemann, R. E., H. J. Cantow, and C. Friedrich, "Interpretation of a new interface-governed relaxation process in compatibilized polymer blends," *Macromolecules* **30**, 5476–5484 (1997).
- Sailer, C., and U. A. Handge, "Melt viscosity, elasticity, and morphology of reactively compatibilized polyamide 6/styrene-acrylonitrile blends in shear and elongation," *Macromolecules* **40**, 2019–2028 (2007).
- Schulze, J. S., J. J. Cernohous, A. Hirao, T. P. Lodge, and C. W. Macosko, "Reaction kinetics of end-functionalized chains at a polystyrene/poly(methyl methacrylate) interface," *Macromolecules* **33**, 1191–1198 (2000).
- Sun, Y. J., R. J. G. Willemsse, T. M. Liu, and W. E. Baker, "*In situ* compatibilization of polyolefin and polystyrene using Friedel-Crafts alkylation through reactive extrusion," *Polymer* **39**, 2201–2208 (1998).
- Sundararaj, U., and C. W. Macosko, "Drop breakup and coalescence in polymer blends: The effects of concentration and compatibilization," *Macromolecules* **28**, 2647–2657 (1995).
- Takeda, Y., H. Keskkula, and D. R. Paul, "Effect of polyamide functionality on the morphology and toughness

- of blends with a functionalized block copolymer," *Polymer* **33**, 3173–3181 (1992).
- Tselios, C., D. Bikiaris, V. Maslis, and C. Panayiotou, "*In situ* compatibilization of polypropylene-polyethylene blends: A thermomechanical and spectroscopic study," *Polymer* **39**, 6807–6817 (1998).
- Van Hemelrijck, E., P. Van Puyvelde, C. W. Macosko, and P. Moldenaers, "The effect of block copolymer architecture on the coalescence and interfacial elasticity in compatibilized polymer blends," *J. Rheol.* **49**, 783–798 (2005).
- Van Hemelrijck, E., P. Van Puyvelde, S. Velankar, C. W. Macosko, and P. Moldenaers, "Interfacial elasticity and coalescence suppression in compatibilized polymer blends," *J. Rheol.* **48**, 143–158 (2004).
- Velankar, S., P. Van Puyvelde, J. Mewis, and P. Moldenaers, "Effect of compatibilization on the breakup of polymeric drops in shear flow," *J. Rheol.* **45**, 1007–1019 (2001).
- Velankar, S., P. Van Puyvelde, J. Mewis, and P. Moldenaers, "Steady-shear rheological properties of model compatibilized blends," *J. Rheol.* **48**, 725–744 (2004).
- Wang, J., and S. Velankar, "Strain recovery of model immiscible blends: Effects of added compatibilizer," *Rheol. Acta* **45**, 741–753 (2006).
- Wildes, G. S., T. Harada, H. Keskkula, D. R. Paul, V. Janarthanan, and A. R. Padwa, "Synthesis and characterization of an amine-functional SAN for the compatibilization of PC/ABS blends," *Polymer* **40**, 3069–3082 (1999).
- Yin, Z., C. Koulic, C. Pagnoulle, and R. Jerome, "Probing of the reaction progress at a PMMA/PS interface by using anthracene-labeled reactive PS chains," *Langmuir* **19**, 453–457 (2003).
- Yoon, Y., A. Hsu, and L. G. Leal, "Experimental investigation of the effects of copolymer surfactants on flow-induced coalescence of drops," *Phys. Fluids* **19**, 023102 (2007).
- Zhang, H., R. A. Weiss, L. E. Kuder, and D. Cangiano, "Reactive compatibilization of blends containing liquid crystalline polymers," *Polymer* **41**, 3069–3082 (2000).